LAWRENCE
LIVERMORE
NATIONAL
LABORATORY

LLNL-JRNL-485341

The feasibility of isobaric suppression of 26Mg via post-accelerator foil stripping for the measurement of 26Al.

S. J. Tumey, T. A. Brown, R. C. Finkel, D. H. Rood

June 2, 2011

Nuclear Instruments and Methods in Physics Research B

Disclaimer

The feasibility of isobaric suppression of ^{26}Mg via post-accelerator foil stripping for the measurement of ^{26}Al.

Scott J. Tumey[1], Thomas A. Brown[1], Robert C. Finkel[2], Dylan H. Rood[1,3]

1 – Center for Accelerator Mass Spectrometry, Lawrence Livermore National Laboratory, P.O. Box 808, L-186, Livermore, CA 94551, USA

2 – Department of Earth and Planetary Science, University of California, 307 McCone Hall, Berkeley, California, USA

3 – Earth Research Institute, University of California, Santa Barbara, CA 93196, USA

Abstract

Most accelerator mass spectrometry measurements of ^{26}Al utilize the Al^- ion despite lower source currents compared with AlO- since the stable isobar ^{26}Mg does not form elemental negative ions. A gas-filled magnet allows sufficient suppression of ^{26}Mg thus enabling the use of the more intense $^{26}AlO^-$ ion. However, most AMS systems do not include a gas-filled magnet. We therefore explored the feasibility of suppressing ^{26}Mg by using a post-accelerator stripping foil. With this approach, combined with the use of alternative cathode matrices, we were able to suppress ^{26}Mg by a factor of twenty. This suppression was insufficient to enable the use of $^{26}AlO^-$, however further refinement of our system may permit its use in the future.

1. Introduction

Cosmogenically-produced ^{26}Al is widely used in the Earth sciences for surface exposure and burial age dating. Due to its long half-life (~705,000 yr), accelerator mass spectrometry (AMS) is the method of choice for measurement of ^{26}Al at naturally-occurring levels. One normally selects the most intensely produced negative ion associated with the isotope of interest to provide the most efficient AMS measurements. In the case of aluminum oxide, which is the preferred target material for ^{26}Al AMS, AlO^- is by far the most intense negative ion, but has not been traditionally used because of the presence of the ^{26}Mg isobar. Since Mg does not produce stable elemental negative ions, Al^- is typically employed to achieve acceptable isobaric suppression of ^{26}Mg. The beam currents obtained for Al^- are much lower than for AlO^-, typically by a factor of ten to twenty. These lower beam currents limit the total number of ^{26}Al counts that can be measured and thus the overall precision of ^{26}Al AMS. It was recently demonstrated [1,2] that ^{26}Al could be effectively distinguished from ^{26}Mg based on the ion trajectories caused by differences in mean charge state in a gas-filled magnet which enables the use of AlO^- rather than Al^-. However, for many AMS facilities, a gas-filled magnet is not feasible due to logistical (e.g., space) or financial concerns.

There are several potential alternatives to a gas-filled magnet for suppressing ^{26}Mg. First, a thin foil can be placed before a high-energy analyzing magnet of an AMS system. The differential energy loss induced by the foil will cause ^{26}Al and ^{26}Mg to exit the magnet with slightly different trajectories. Appropriate positioning of the image slits of the magnet can maximize the transmission of ^{26}Al while minimizing the transmission of ^{26}Mg. The acceptance of ^{26}Al and rejection of ^{26}Mg increase logarithmically with increasing foil thickness as the demonstrated in Figure 1. It is important to note that these acceptance and rejection factors, which were calculated using output from the SRIM code [3], represent the ideal case where the post-magnet separation between the ^{26}Al and ^{26}Mg beams is governed only by their energy loss and energy straggling. In reality, the resolution between ^{26}Al and ^{26}Mg is determined by the ion optical properties of the system which includes beam spreading caused by angular straggling in the foil.

The post-accelerator degrader foil method has been successfully used to suppress ^{36}S for the measurement of ^{36}Cl [4,5]. There are several important differences between the ^{26}Al-^{26}Mg and ^{36}Cl-^{36}S isobar systems. First, because the relative difference in atomic numbers is greater for ^{26}Al and ^{26}Mg, the differential energy loss, and subsequent beam resolution, will be greater than for ^{36}Cl and ^{36}S. Furthermore, resolution-degrading effects such as angular straggling will be smaller for ^{26}Al-^{26}Mg than for ^{36}Cl-^{36}S. Unfortunately, ^{26}Mg is ~50,000 times more abundant in the Earth's crust than ^{36}S [6] which necessitates a much greater suppression factor to allow measurement of ^{26}Al using the AlO^- ion.

The post-accelerator degrader foil method for suppressing ^{26}Mg can be augmented by taking advantage of the differential stripping yield between Mg and Al. By

selecting an appropriate terminal voltage and charge state combination, the stripping yield of Al relative to Mg can be maximized as illustrated in Figure 2 which shows stripping yields calculated using the Sayer formalism [7]. Unfortunately, at the terminal voltage of 7.0 MV for which Figure 2 was calculated, the highest values of the Al/Mg stripping yield ratio can only be attained at the expense of lower overall Al yield. However this approach can still be useful if the reduction in Al stripping yield is less than the factor of 10-20 enhancement in source output associated with AlO^- versus Al^-. It is important to note that fully-stripping Al to the 13+ charge state would completely suppress the Mg isobar, but as Figure 2 demonstrates, the stripping yield is sufficiently low so as to effectively negate the higher AlO^- current.

We employed both of these methods in order to test whether more efficient AMS measurements of ^{26}Al are possible with AlO^- without the need for a gas-filled magnet. To further suppress ^{26}Mg we also searched for alternative cathode materials that possess intrinsically lower level of Mg than the aluminum or stainless steel targets that we typically use in our ion source.

2. Experimental

All experiments were conducted on the Lawrence Livermore National Laboratory AMS system [8]. A ladder containing five arc-evaporated carbon foils (ACF-Metals, USA) ranging in thickness from 10 to 200 $\mu g/cm^2$ was installed in between the first and second high-energy analyzing magnets which was determined to be the optimum placement. With this ladder we were able to determine the thickness of foil that yielded the best separation between ^{26}Al and ^{26}Mg following the second analyzing magnet. This was accomplished by optimizing the system tune for each foil and selecting the thickest foil that yielded no significant transmission losses. We then assessed the separation between ^{26}Al and ^{26}Mg by scanning the second analyzing magnet and measuring counts of each isotope in our final detector normalized to ^{27}Al current measured in the off-axis Faraday cup located between the two analyzing magnets. During this scan, the image slits of the second magnet were narrowly set to achieve Gaussian-like scan profiles thus yielding accurate representation of the beam distributions. The final detector is a multi-anode gas ionization chamber which allows for effective separation of ^{26}Al and ^{26}Mg based on differential energy loss. The detector resolution can be tuned for a particular ion energy by adjusting the gas pressure in the detector.

To assess the suppression of ^{26}Mg based on relative stripping yield we tested four different combinations of terminal voltage and charge states (both post-accelerator and post-foil) as indicated in Table 1. For each system configuration, we measured Al transmission by comparing $^{27}Al^{N+}$ current measured between the two high energy analyzing magnets to $^{27}Al^-$ or $^{27}AlO^-$ current injected into the accelerator, corrected for the transmission lost due to the gridded lens in the accelerator. We also

measured ^{26}Mg counts in our detector normalized to $^{27}Al^{N+}$ current measured in the off-axis Faraday cup located between the two analyzing magnets.

To evaluate the Mg content of a various materials we pressed ultra-high purity metal powders into bored-out versions of our standard cathodes. The powders (all Puratronic grade, Alfa-Aesar, USA) were compacted using a special press that effectively formed the front surface of the cathode into the same geometry as our standard cathodes. Samples of aluminum oxide blank material (also Puratronic grade) were then mixed in approximately a 1:5 ratio (by mass) with each of the metal powders and then loaded into the corresponding cathode. We measured $^{26}Mg/^{27}Al$ ratios in each of these samples as counts in our detector normalized to current in the off-axis Faraday cup. These measurements were performed using configuration B indicated in Table 1, but exceedingly high ^{26}Mg count rates for some materials required us to attenuate the beam using slits located immediately after the source.

3. Results & Discussion

The results of the investigation of alternative cathode materials are presented in Table 2. Since these measurements were performed with an attenuated beam, the $^{26}Mg/^{27}Al$ ratios can only be considered a relative measure of the Mg content of the various cathode materials. Nearly all materials possessed lower levels of Mg than our normal stainless steel cathodes, and iron and cobalt yielded the lowest $^{26}Mg/^{27}Al$ ratios. Surprisingly, silver appeared to have the highest level of Mg impurity. The cobalt powder that we used was so voluminous that it was difficult to press efficiently into the modified cathodes, therefore iron powder was used for all subsequent measurements.

Table 3 presents the results of differential stripping yield measurements for the four different system configurations that we investigated. To compare the measured $^{26}Mg/^{27}Al$ ratio of the system configurations investigated, the $^{27}Al^{N+}$ current is expressed as particle-nanoCoulombs (pnC). The expected trend of increasing Al/Mg stripping yield ratio yielding a lower measured $^{26}Mg/^{27}Al$ ratio was observed, however the agreement was not perfectly linear. For example, based on the relative stripping yield ratios, one would expect that configuration C would produce a $^{26}Mg/^{27}Al$ ratio approximately three times lower than configuration B rather than the factor of 8.5 which was observed. This discrepancy may be a result of the semi-empirical nature of the Sayer formula [7] that was used to calculate the stripping yield, or may indicate transmission losses in the system. Further experiments are required to answer this question.

Configuration A represents our standard operating conditions that we routinely use for measurement of ^{26}Al. This configuration yields the highest Al transmission and since Mg does not form negative ions, the effective $^{26}Mg/^{27}Al$ ratio is zero. We obtained approximately 10 to 20 times higher source output for configurations B, C,

and D which use the $^{26}AlO^-$ molecular ion. However, for configurations B and C the ^{26}Mg count rates were high enough to cause significant dead time in our detector and required us to attenuate the beam in order to perform measurements. Attenuation was achieved by winding in slits immediately after the source so that both Mg and Al beams were attenuated by the same proportion. Configuration D yielded an acceptable suppression of ^{26}Mg (i.e., no beam attenuation was required), but the overall Al stripping yield was sufficiently low so as to offset the gain in beam current from using the molecular ion.

The separation between ^{26}Al and ^{26}Mg after the second high-energy analyzing magnet caused by differential energy loss in the post-accelerator degrader foil is illustrated in Figure 3. The calculations indicate that the ^{26}Mg count rate in the detector could be reduced by at least a factor of five by setting the magnet field for the peak of the ^{26}Al beam and appropriately positioning the magnet image slits to collimate the beam at the intersection point between ^{26}Al and ^{26}Mg. Clearly, the measured peak widths are larger than the SRIM calculations predict. One possible reason for this could be inaccuracy in the energy straggling calculated by SRIM in this energy range. For comparison, we calculated the energy straggling using an alternative method proposed by Yang [9]. Using the Yang formula yields a value for energy straggling that is ~50% higher than the value calculated by SRIM, however this difference is not enough to fully explain the observed distributions. These calculations are based purely on the differential energy loss between ^{26}Al and ^{26}Mg and do not take into account angular straggling or thickness inhomogeneities associated with the degrader foil, which are the most likely explanations for the wider than expected distributions. As a result, only a factor of two suppression in ^{26}Mg was achieved.

4. Conclusion

Our results show that while some suppression of ^{26}Mg can be achieved using alternative methods, a gas-filled magnet is still required to perform ^{26}Al AMS measurements when injecting the $^{26}AlO^-$ negative ion. We achieved a factor of two suppression of ^{26}Mg by employing a post-accelerator degrader foil. A factor of five suppression factor is theoretically possible, but angular straggling in the foil limited the separation between the ^{26}Al and ^{26}Mg beams. Some of this straggling can be attributed to non-uniformity in the thickness of the foil, so slightly better ^{26}Mg suppression could be achieved by using either diamond-like carbon or silicon nitride foils. We achieved a further factor of ten suppression in ^{26}Mg by using high-purity iron rather than stainless steel for the cathode material. Further investigation may reveal other materials with even lower levels of Mg.

We demonstrated that Mg could be further suppressed by selecting a charge state and terminal voltage combination that gives a favorable Al/Mg differential stripping yield. However, in order to reduce ^{26}Mg count rates to sufficiently low levels to achieve acceptable detector dead-times, we had to operate with system parameters

that yielded unacceptably low Al stripping yield. However, the analog-to-digital conversion time of our electronics system is currently ~40 μs. We are currently in the process of implementing faster electronics which will allow us to process higher count rates in our detector. This may enable us to select a charge state and terminal voltage combination that gives acceptably high Al stripping yield while suppressing Mg sufficiently to enable measurement of ^{26}Al by injecting $^{26}AlO^-$.

Acknowledgements

The authors wish to thank Martin Suter for his helpful discussions regarding this work and John Stone for providing the zinc cathodes that were used in the investigation of alternative materials. This work performed under the auspices of the U.S. Department of Energy by Lawrence Livermore National Laboratory under Contract DE-AC52-07NA27344.

References

[1] – L.K. Fifield, S.G. Tims, L.G. Gladkis, C.R. Morton, Nucl. Instr. Meth. Phys. Res. B 259 (2007) 178.

[2] – A. Arazi, T. Faestermann, J.O. Fernandez Niello, D. Frischke, K. Knie, G. Korschinek, H.J. Maier, E. Richter, G. Rugel, A. Wallner, Nucl. Instr. Meth. Phys. Res. B 223–224 (2004) 259.

[3] – J.F. Ziegler, Nucl. Inst. Meth. Phys. Res. B 219-220 (2004) 1027.

[4] – M.G. Klein, A. Gottdang, D.J.W. Mous, D.L. Bourlès, M. Arnold, B. Hamelin, G. Aumaître, R. Braucher, S. Merchel, F. Chauvet, Nucl. Instr. Meth. Phys. Res. B 266 (2008) 1828.

[5] – M. Arnold, S. Merchel, D.L. Bourlès, R. Braucher, L. Benedetti, R.C. Finkel, G. Aumaître, A. Gottdang, M. Klein, Nucl. Instr. Meth. Phys. Res. B 268 (2010) 1954.

[6] – W.M. Haynes, ed., CRC Handbook of Chemistry and Physics, 92nd Edition (Internet Version 2012), CRC Press/Taylor and Francis, Boca Raton, FL.

[7] - R.O. Sayer, Revue De Physique Appliquee 12 (1977) 1543.

[8] – J.R. Southon, M.W. Caffee, J.C. Davis, T.L. Moore, I.D. Proctor, B. Schumacher, J.S. Vogel, Nucl. Instr. Meth. Phys. Res. B 52 (1990) 301.

[9] – Q. Yang, D.J. O'Connor, Z. Wang, Nucl. Instr. Meth. Phys. Res. B 61 (1991) 149.

Tables

Table 1. Summary of the key system parameters for the four system configurations that we investigated. The parameters of system configuration A reflect our normal operating conditions. All configurations use a 4 μg/cm2 carbon foil as the terminal stripper.

System Configuration	Injected Ion	Terminal Voltage (MV)	Post-accelerator charge state	Post-foil charge state
A	$^{26}Al^-$	7.000	7+	N/A
B	$^{26}Al^{16}O^-$	7.353	7+	11+
C	$^{26}Al^{16}O^-$	7.353	7+	12+
D	$^{26}Al^{16}O^-$	7.353	9+	12+

Table 2. Results of $^{26}Mg/^{27}Al$ measurements of various cathode materials. Each value is the weighted mean of at least three repeated measurements and the quoted uncertainty is the greater of the propagated counting statistics or the weighted standard error of the mean. Each cathode material/bulking agent combination was tested on at least two different physical samples with the exception of Zn/Zn.

Cathode Material	Bulking agent	Measured $^{26}Mg/^{27}Al$ (counts/pC)
Stainless Steel	Nb	0.550 ± 0.080
		0.454 ± 0.073
	Ag	3.40 ± 0.20
		4.56 ± 0.23
Cu	Cu	0.323 ± 0.062
		0.465 ± 0.074
Fe	Fe	0.036 ± 0.021
		0.043 ± 0.021
Co	Co	0.084 ± 0.032
		0.024 ± 0.017
Mo	Mo	0.91 ± 0.12
		0.192 ± 0.048
		0.140 ± 0.040
Ni	Ni	0.137 ± 0.037
		0.120 ± 0.038
Ag	Ag	0.838 ± 0.032
		0.648 ± 0.088
Nb	Nb	0.299 ± 0.060
		0.235 ± 0.050
W	W	0.222 ± 0.041
		0.069 ± 0.028
Ta	Ta	0.554 ± 0.081
		0.156 ± 0.043
		0.393 ± 0.068

		0.143 ± 0.041
Zn	Zn	0.360 ± 0.066

Table 3. Comparison of the calculated Al stripping yield and Al/Mg stripping yield ratio to the measured Al transmission and $^{26}Mg/^{27}Al$ ratio. Since Mg does not form elemental negative ions, the $^{26}Mg/^{27}Al$ ratio for configuration A is effectively zero. Calculations are based on the formalism developed by Sayer [7] using a foil stripper in the terminal of the accelerator.

	Calculated		Measured	
System Configuration	Al Stripping Yield	Al/Mg Stripping Yield Ratio	Al Transmission	$^{26}Mg/^{27}Al$ (counts/pnC)
A	36.6%	1.14	31.9%	N/A
B	9.57%	2.30	6.30%	284
C	4.54%	7.55	2.23%	33.2
D	0.157%	15.0	0.292%	5.55

Figure Captions

Figure 1. Plot showing the relationship between the fraction of ^{26}Al ions that would be transmitted and the fraction of ^{26}Mg ions that would be rejected by the second high-energy analyzing magnet as a function of the thickness of a degrader foil placed before the magnet. Calculations are based on the differential energy loss of 56.04 MeV incident ions as calculated by SRIM-2008.04 [3] and assume that the magnet image slits are set at the point where the ^{26}Al and ^{26}Mg beam profiles would intersect.

Figure 2. Plot showing the post-accelerator stripping yields of ^{26}Al and ^{26}Mg and the Al/Mg stripping yield ratio resulting from the injection of $^{26}Al^-$ and $^{26}Mg^-$ respectively. Calculations are based on the formalism developed by Sayer [7] and assume a terminal voltage of 7.0 MV.

Figure 3. Plot showing the separation of ^{26}Al and ^{26}Mg ions after passing through a 100 ug/cm^2 post-accelerator degrader foil located before the second high-energy analyzing magnet as the magnet field was scanned. These measurements were performed using system configuration D listed in Table 1. Symbols reflect ^{26}Al and ^{26}Mg counts detected in the final detector normalized against ^{27}Al current measured in an off-axis Faraday cup located before the magnet. Lines represent calculated distribution of ^{26}Al and ^{26}Mg ions based on the energy loss predicted by SRIM-2008.04 [3]. The actual energy loss in the foil is 1.144 MeV for ^{26}Mg and 1.278 MeV for ^{26}Al.

Figure 1

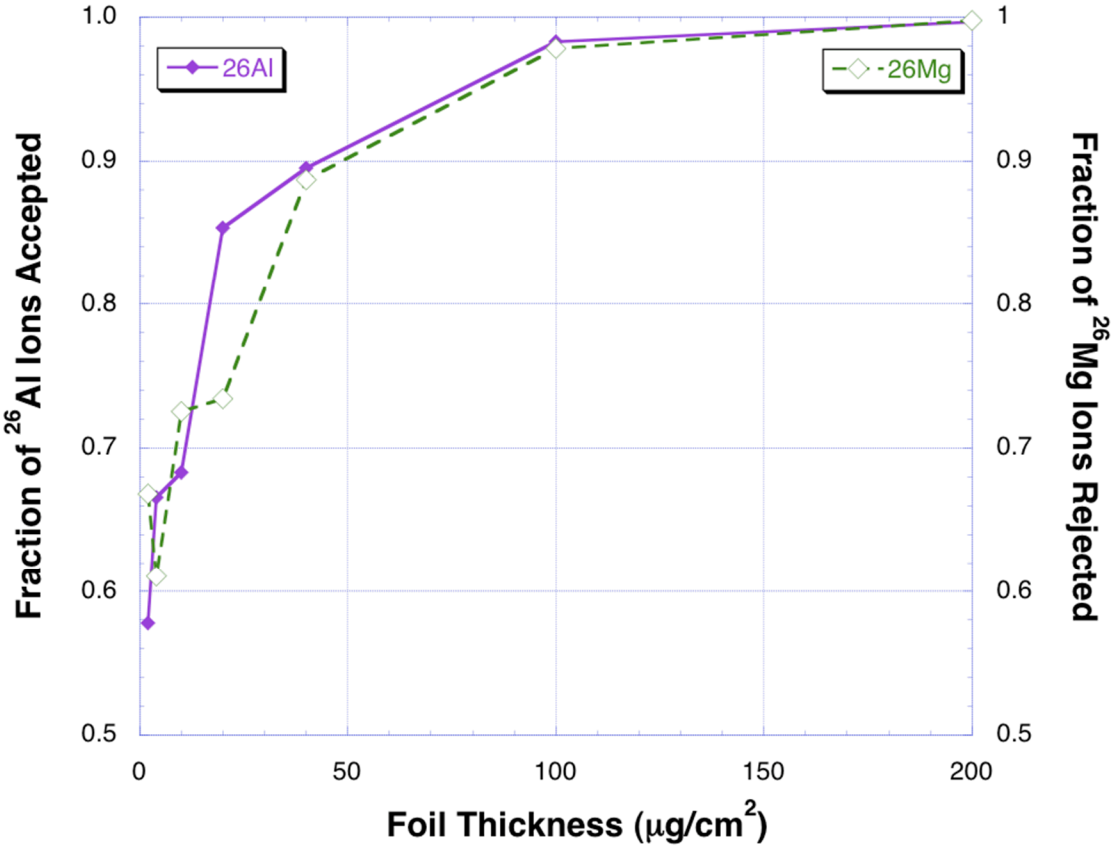
26Al
26Mg
1.0
0.9
0.8
0.7
0.6
0.5
1
0.9
0.8
0.7
0.6
0.5
0
50
100
150
200
Fraction of 26Al Ions Accepted
Fraction of 26Mg Ions Rejected
Foil Thickness (μg/cm2)

Figure 2

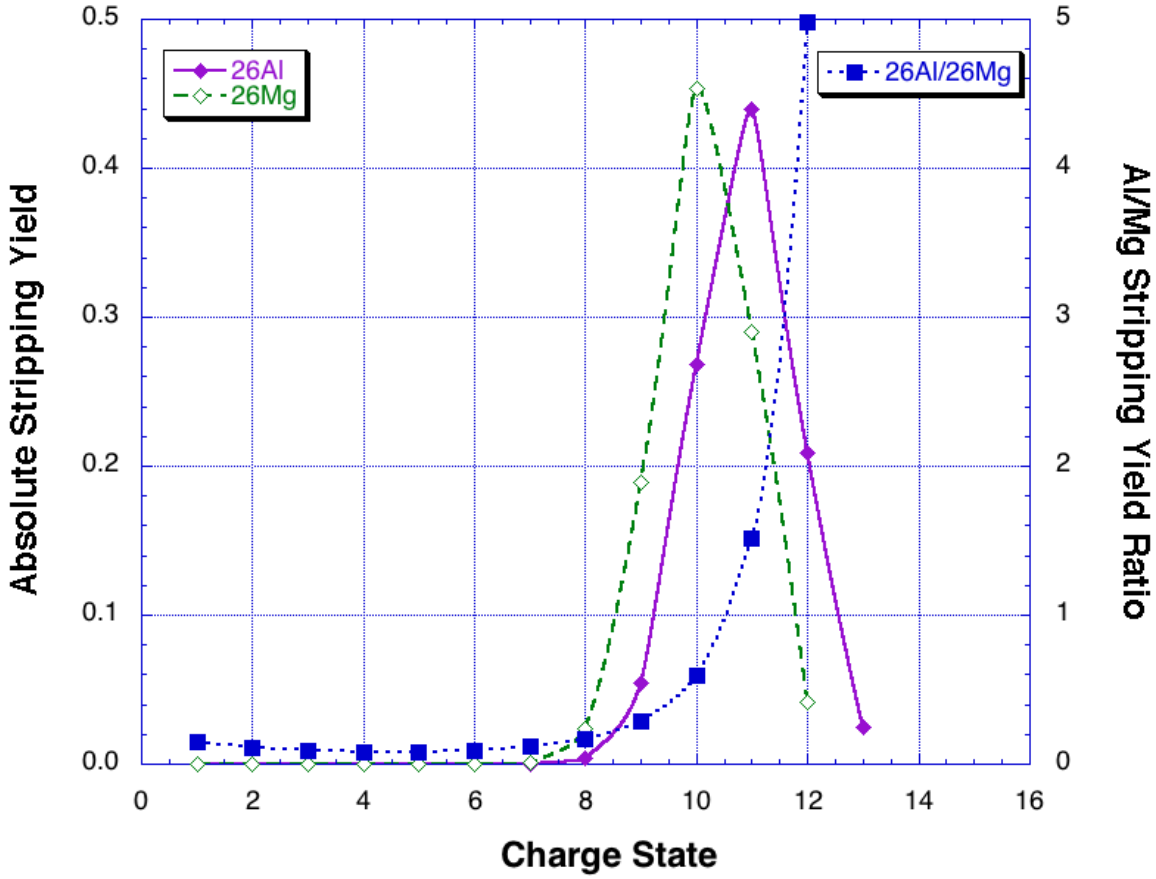
26Al
26Mg
26Al/26Mg
Absolute Stripping Yield
Al/Mg Stripping Yield Ratio
Charge State
0.0
0.1
0.2
0.3
0.4
0.5
0
1
2
3
4
5
0
2
4
6
8
10
12
14
16

Figure 3

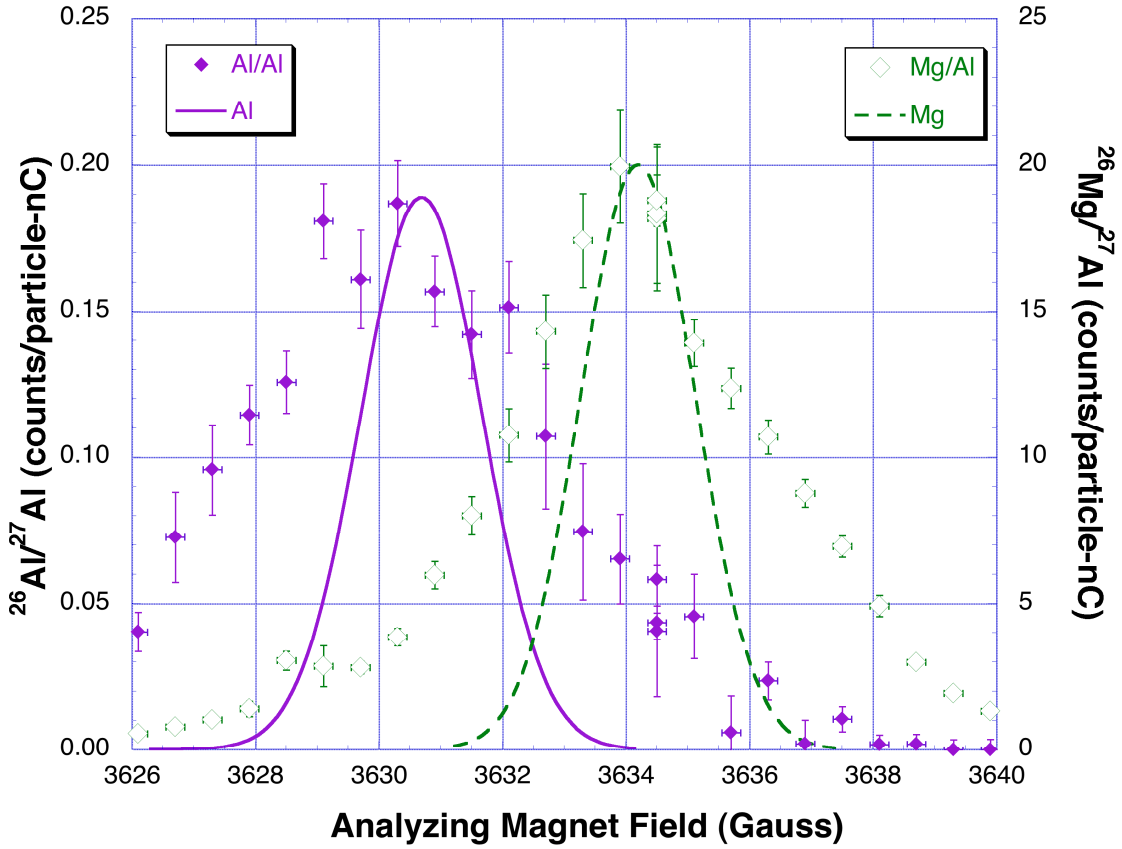
Al/Al
Al
Mg/Al
Mg
0.25
0.20
0.15
0.10
0.05
0.00
25
20
15
10
5
0
3626
3628
3630
3632
3634
3636
3638
3640
$^{26}Al/^{27}Al$ (counts/particle-nC)
$^{26}Mg/^{27}Al$ (counts/particle-nC)
Analyzing Magnet Field (Gauss)